Check for updates

Original Article

Biofpr Biofuels Bioproducts & Biorefining

# Catalytic conversion of bioethanol over cobalt and nickel-doped HZSM-5 zeolite catalysts

**Ifeanyi Michael Smarte Anekwe,** School of Chemical and Metallurgical Engineering, University of the Witwatersrand, Johannesburg, South Africa
**Bilainu Oboirien,** Department of Chemical Engineering Technology, University of Johannesburg, Johannesburg, South Africa
**Yusuf Makarfi Isa,** School of Chemical and Metallurgical Engineering, University of the Witwatersrand, Johannesburg, South Africa

**Received April 27 2023; Revised July 24 2023; Accepted August 8 2023;**
**View online 14 September 2023, at Wiley Online Library (wileyonlinelibrary.com);**
**DOI: 10.1002/bbb.2536; *Biofuels, Bioprod. Bioref.* 18:686–700 (2024)**

Abstract: This study focuses on the use of H-ZSM-5 catalyst modified with transition metals for the conversion of ethanol into liquid fuel hydrocarbons. The HZSM-5 catalyst was synthesized hydrothermally, and the transition metal (0.5 wt%) was incorporated by the incipient wetness impregnation method. The synthesized catalysts were tested in a fixed-bed reactor at varying weight hourly space velocities (WHSVs) and temperatures to investigate their effects on the selectivity of the liquid hydrocarbon product. The pure and metal-doped catalysts were characterized using XRD, FTIR, SEM–EDX, PSD, BET, $N_2$ adsorption–desorption, and $NH_3$-TPD. The metal species were evenly dispersed on the catalyst support without affecting the porous framework significantly. The modification did not alter the morphology of the catalyst; however, the particle size was altered slightly. The pore distribution plot confirms the hierarchical porous framework of the catalyst. This unique feature facilitates internal diffusion and accelerates mass transfer, improving the selectivity and distribution of the liquid product. The catalytic evaluation showed ethanol conversion of more than 97% for all catalysts tested. A low space velocity ($5\,h^{-1}$) favored gaseous ($C_1$-$C_4$) hydrocarbons, but more liquid products ($C_5$+) were generated at $12\,h^{-1}$ (at 350 and 400 °C), with metal-doped catalysts showing higher selectivity (>79%). In comparison with the unmodified catalysts, the metal-doped catalysts enhanced the production of aromatics (benzene), with Ni/HZSM-5 showing higher selectivity (>4%). This study showed that the synthesized catalysts are active in the selective production of liquid hydrocarbon and improve the transformation of ethanol to fuel-range hydrocarbons. © 2023 The Authors. Biofuels, Bioproducts and Biorefining published by Society of Industrial Chemistry and John Wiley & Sons Ltd.

Key words: catalyst; ethanol; HZSM-5; cobalt; nickel

Correspondence to: Ifeanyi Michael Smarte Anekwe, School of Chemical and Metallurgical Engineering, University of the Witwatersrand, Johannesburg 2050, South Africa. E-mail: anekwesmarte@gmail.com

SCI where science meets business



© 2023 The Authors. *Biofuels, Bioproducts and Biorefining* published by Society of Industrial Chemistry and John Wiley & Sons Ltd.
This is an open access article under the terms of the Creative Commons Attribution-NonCommercial License, which permits use, distribution and reproduction in any medium, provided the original work is properly cited and is not used for commercial purposes.

## Introduction

The synthesis of ethanol from renewable resources has the potential to make it an essential primary chemical in the petrochemical sector.[1] Bioethanol can be synthesized by fermenting lignocellulosic feedstock such as wood, grasses, and other plant materials without affecting food production.[2] The application of bioethanol directly as a fuel or as a constituent of gasoline blends offers several benefits, including an increased octane rating, extended combustion limits, and reduction of greenhouse gas emissions.[3,4] On the other hand, ethanol, as a fuel, has several limitations, including effects on engines, the need for processes requiring significant energy input, such as distillation to remove water, and low energy density.[5] Due to these limitations, investigations into ethanol enhancement techniques have increased.[6] Some examples are the steam reforming of ethanol to produce $H_2$ or synthesis gas, the synthesis of acetaldehyde and ethylene by dehydration, and the subsequent acid transformation of these substances into chemical building blocks and gasoline, upgrading ethanol to a hydrocarbon suitable for use as a fuel.[7]

Since the 1970s, researchers have studied the conversion of alcohol with zeolites, focusing mainly on lower alcohols.[8] Alcohol conversion using zeolites can produce a wide range of products, and correlations between the transformation of methanol to olefins and ethanol conversion have already been recognized. The transformation of ethanol to ethylene was the main focus of early research,[9] followed by studies on the production of higher hydrocarbons (HCs).[10] The synthesis of polyethylene, ethylene oxide, and dichloroethane requires ethylene. During ethanol transformation, other light olefins are also produced, such as propylene, an essential chemical in the polymer industry, and $C_4$ olefins, which are utilized in processes such as the alkylation of isobutene with isobutane to produce iso-octane. Although they occur in much smaller quantities, other light olefins include light paraffins and aromatics. Hydrocarbons with a carbon number greater than 5, including olefins, paraffins, and aromatics, have desirable fuel properties.[7]

In a recent article, the authors[11] reviewed several works on ethanol-to-hydrocarbon (ETH) conversion over zeolites.[11] It has been shown that HZSM-5 is the best choice for major HC synthesis due to the distribution and stability of the products.[12,13] The HC pool mechanism has also been postulated for the conversion of ethanol to HCs.[14] Other proposed techniques include conventional alkene alkylation accompanied by cracking of higher olefins. This mechanism has been employed to build simpler kinetic models[15] and a radical-based process.[16] On the other hand, the acid-catalyzed transformation of ethanol to HCs on HZSM-5 remains a topic of discussion. Post-synthetic treatments are usually carried out to enhance the efficiency of the catalyst. Post-synthesis modifications of zeolites include impregnation and ion exchange with metal salts to produce a metal-doped zeolite, promoting with phosphorus, alkali treatment, and vapor deposition. These treatments are expected to lead to either an improvement in hydrothermal durability, a reduction in deactivation, an increase in performance, or specificity for a particular product category.[17,18]

The study of metal-modified zeolites is the focus of this work. The method by which zeolites are treated substantially impacts the metal concentration of the catalyst. For instance, in hydrocracking, the metal species and the acid function play a delineated and discrete with specific role: the alkane is dehydrogenated by the metal, producing an olefin. The olefin is then protonated at the acidic site, leading to isomerization and cracking of the carbenium ion. Finally, the process is repeated in reverse order.[19] However, in a large number of processes the role of the metal is not properly recognized or described.[20] The influence of Ni has been revealed in catalytic cracking but the addition of transition metals such as Ni gave remarkable results in the aromatization and cracking of light alkenes and alkanes.[21,22] A previous study discussed nickel-catalyzed reaction pathways on various supports.[23] This is commonly applied for olefin oligomerization, especially ethylene oligomerization, to linear olefins, where the active species are recognized as $Ni^{2+}$ ions. In catalytic cracking, there has also been speculation about the properties of iron modification, which could increase activity.[24]

In the ETH transformation, the introduction of metals into HZSM-5 has been investigated with nickel,[25] iron,[26,27] zinc, and gallium,[28] molybdenum,[29] and rare earth metals.[30] It has been found that the addition of nickel to a catalyst for the transformation of ethanol to higher HCs can increase its hydrothermal stability. This is achieved through nickel's ability to influence the acid site's equilibrium, consequently influencing product distribution. The incorporation of gallium into HZSM-5 is reported to have the opposite effect, leading to an increase in the production of aromatics, and the introduction of iron into HZSM-5 is reported to limit the synthesis of aromatics and paraffins. These effects can be attributed to either inhibiting or facilitating hydrogen transfer processes. However, the effects of metal incorporation on catalyst features, reaction process and product specificity, particularly $C_5$+ specificity, are rarely discussed. It can be challenging to determine how the presence of metal affects the efficiency of a catalyst based only on published research, as different reaction parameters, varying metal concentrations, and deactivation can complicate the

© 2023 The Authors. *Biofuels, Bioproducts and Biorefining* published by Society of Industrial Chemistry and John Wiley & Sons Ltd.


19321031, 2024, 3, Downloaded from https://scijournals.onlinelibrary.wiley.com/doi/10.1002/bbb.2536 by South African Medical Research, Wiley Online Library on [27/08/2024]. See the Terms and Conditions (https://onlinelibrary.wiley.com/terms-and-conditions) on Wiley Online Library for rules of use; OA articles are governed by the applicable Creative Commons License

19321031, 2024, 3, Downloaded from https://scijournals.onlinelibrary.wiley.com/doi/10.1002/bbb.2536 by South African Medical Research, Wiley Online Library on [27/08/2024]. See the Terms and Conditions (https://onlinelibrary.wiley.com/terms-and-conditions) on Wiley Online Library for rules of use; OA articles are governed by the applicable Creative Commons License

process.[13,31] Moreover, to the best of our knowledge, no study has investigated the impact of metal loadings, specifically Ni and Co, on a non-commercial novel ZSM-5 catalyst with Si/Al of 40 for the conversion of ethanol to $C_5$+ hydrocarbons.

To this end, this study aimed to increase product distribution and selectivity of liquid ($C_5$+) HC, which can be obtained from the catalytic conversion of ethanol by modifying ZSM-5 while adjusting both the reaction temperature and space velocities. The ZSM-5 zeolite catalyst active in converting low alcohol into hydrocarbon was therefore synthesized and modified with nickel and cobalt to enhance liquid product selectivity. To investigate the effects of metal doping on the catalytic activities of a zeolite catalyst, a methodological approach was used to test the incorporation of Co and Ni in a newly synthesized HZSM-5 catalyst. The catalyst properties were investigated using a thorough characterization process to study the effects of metal promotion on the ZSM-5 support. The catalyst study considered whether a metal modification is best suited to improve the selectivity of liquid products in ETH conversion.

# Materials and methods

## Materials

The chemicals used for this study included $(Na_2O)SiO_2.H_2O$ (a silica source), $Al_2(SO_4)_3.18H_2O$ (a source of aluminium), TPABr – $C_{12}H_{28}BrN$ (a structure-directing agent, SDA), NaOH (97%), $H_2SO_4$ (98%) (for pH adjustment), $NH_4NO_3$ (for ion exchange), transition metal precursors: $Ni(NO_3)_2{\cdot}6H_2O$ and $Co(NO_3)_2{\cdot}6H_2O$, and $C_2H_5OH$ was used as the feedstock. All chemicals were analytical grade and obtained from Sigma-Aldrich, Darmstadt, Germany. A stainless-steel hydrothermal reactor (HTR) with a Teflon cup of 200 mL with a 150 mL working volume was used for catalyst preparation.

## Methods

### Synthesis of transition metal-doped HZSM-5

The ZSM-5 catalyst support was fabricated using the hydrothermal method based on the molar ratio *10*$Na_2O$:*40*$SiO_2$:*1.0*$Al_2O_3$:*10.5*TPABr:*3740.6*$H_2O$. The first solution consisted of NaOH and silica source $(Na_2O)SiO_2.H_2O$ dissolved in deionized water. The structure-directing agent, TPABr, was dissolved in deionized $H_2O$ and was denoted as solution 2. The third solution contained the required amount of aluminium source, aluminium sulfate, dissolved in deionized $H_2O$ while stirring at ambient temperature. Solutions 1 and 2 were mixed under continuous agitation to hydrolyze the components of the mixture thoroughly. After 1 h of agitation, solution 3 was added to the mixture and stirred vigorously at 2000 rpm for 5 h until a homogenous gel mixture was obtained. The initial pH of the gel was stabilized to final pH of 10.73 using 3 mL of sulfuric acid (98% conc.). The final solution (in gel form) was allowed to age for 12 h at room temperature and subsequently transferred into a Teflon-lined stainless-steel reactor for hydrothermal crystallization under autogenous pressure at 180 °C for 24 h. After the crystallization phase, the solid product was cooled to room temperature, recovered by filtration, and thoroughly washed with deionized $H_2O$. The solid product obtained was dried at 110 °C overnight and then calcined at 550 °C for 3 h to eliminate the organic template to obtain Na-ZSM-5. Following the calcination, the Na-ZSM-5 was ion-exchanged for 2 h with a 1 mol $L^{-1}$ solution of $NH_4NO_3$ at 80 °C at 10 mL $g^{-1}$. After the ion exchange, the sample was filtered and washed with deionized $H_2O$ and dried overnight at 110 °C to obtain $NH4^+$-ZSM-5. The ion-exchange method will be repeated twice. The recovered $NH4^+$-ZSM-5 was calcined at 550 °C for 6 h to break down the ammonium ions and produce a hydrogen form of ZSM-5 (HZSM-5).

The catalyst was modified using transition metals (M = Co and Ni) at 0.5 wt% through incipient wetness impregnation, dried overnight, and calcined at 550 °C for 6 h. The transition metal-modified ZSM-5 were denoted M/HZSM-5, where M represents the transition metal.

The catalytic activity of Ni and Co catalysts supported on ZSM-5 zeolites was evaluated at 350–400 °C and a weight hourly space velocity (WHSV) of 5–12 $h^{-1}$. The catalyst bed was supported using glass beads and 0.045 g of glass wool. Ethanol was used as the feedstock for the reaction. Conversion (X) and product selectivity (Si) were deduced as per Sun *et al.*[32]

### Catalyst and product characterization

Powder X-ray diffraction (XRD) spectra of the parent and transition metal doped ZSM-5 were studied using an X-ray diffractometer (Bruker D2 phaser diffractometer) equipped with Cu K radiation ($\lambda$ = 1.54184 Å), the crystallinity of the catalyst was analyzed in 2θ = 0 – 90°. $N_2$ adsorption–desorption studies were conducted on degassed materials at 300 °C for 10 h with a Quantachrome instrument: Autosorb iQ Station 3 (Anton Paar, VA, USA). The Brunauer–Emmett–Teller (BET) equation was used to calculate the surface area of the samples being studied. The Barrett–Joyner–Halenda (BJH) method and the $N_2$ adsorption isotherm were used to calculate the pore volume and diameter. The morphology of the catalyst and the elemental composition were determined using a Ziess Sigma 300 VP, fitted with a field emission gun


© 2023 The Authors. *Biofuels, Bioproducts and Biorefining* published by Society of Industrial Chemistry and John Wiley & Sons Ltd.

for the scanning electron microscope (SEM) and an Oxford Instruments x-act PentaFET Precision Energy-dispersive X-ray spectroscopy (EDS). The Malvern instrument was employed to obtain the particle size distribution (PSD) data. $NH_3$-TPD analysis was conducted using an AutoChem II 2920 chemisorption analyzer to determine catalyst acidity. Liquid HCs were analyzed using a YL6500 gas chromatography (GC) system.

## Results and discussion

### X-ray powder diffraction

The XRD patterns of the parent and metal-doped HZSM-5 catalyst are shown in Fig. 1. In comparison with the standard sample, the characteristic peaks at 2θ = 7.97°, 8.88°, 14.81°, 23.14°, 24.00°, and 24.49° were attributed to planes (101), (020), (301), (501), (303), and (133) of the zeolite crystal with MFI framework (JCPDS 96-154-02468). The existence of peaks in the ranges 2θ = 7–10° and 22–25° confirmed the presence of characteristic HZSM-5 peaks in all catalysts.[33] The XRD pattern of synthesized HZSM-5 was examined, and it was evident that the framework of ZSM-5 was successfully retained despite the introduction of metals. Hence, the addition of metal did not show any significant alteration. Both metal-coated catalysts retained the structure and the crystallinity of their respective parent catalysts. In these XRD peaks, which correlate with a well-crystallized MFI framework, no other peaks belonging to other phases were identified. This means that the Ni and Co metal species were uniformly distributed on the support and that any metal oxide was very small and undetectable. Another work has reported no noticeable peaks within the angles examined, suggesting the absence of metal oxide, the presence of doped metal in small amounts, or an unusually uniform distribution of the incorporated metal.[34]

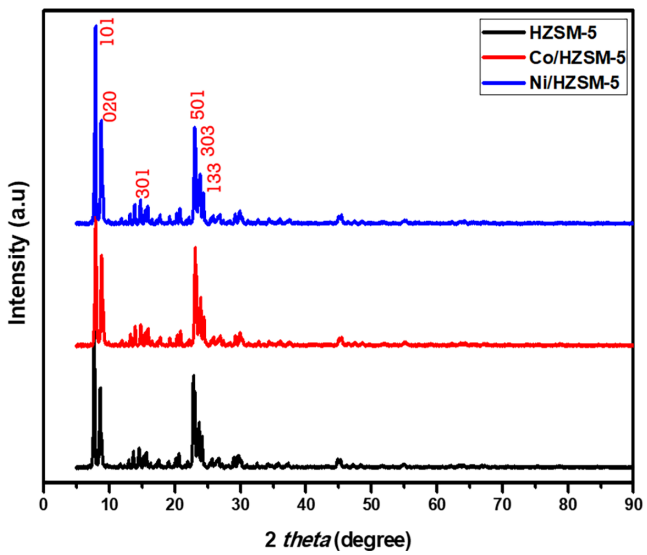


Figure 1. X-ray diffraction powder patterns of the parent HZSM-5, Co/HZSM-5 and Ni/ZSM-5 catalysts.

### Fourier-transform infrared spectroscopy (FTIR)

The FTIR spectra of ZSM-5 and metal-doped ZSM-5 are shown in Fig. 2 and cover the 400–4000 $cm^{-1}$ range. The internal tetrahedral units $AlO_4^-$ and $SiO_4^{4-}$ are responsible for the vibration that produces the peak at 440 $cm^{-1}$.[35] The five-membered rings explain the absorption peak found at 543 $cm^{-1}$.[36] The asymmetric stretching vibrations of the internal and external bonds of $TO_4$ are responsible for the absorption peaks at 791 $cm^{-1}$ and 1218 $cm^{-1}$,[37,38] and the peak at 1633 $cm^{-1}$ indicates the presence of hydroxyl groups ($OH^-$) of absorbed $H_2O$ on the ZSM-5 surface.[39] Confirmation that the calcination technique was successful and that appropriate amounts of template molecules were eliminated from the zeolite structure is provided by a faint peak at 2870–2990 $cm^{-1}$. This peak is due to the stretching absorption bonds of C-H. The bands at 3615 $cm^{-1}$ and 3681 $cm^{-1}$, respectively, are due to the vibration of bonds that defined the internal tetrahedral Si-OH-Al and terminal Al-OH groups, which denote the solid Brønsted acid sites (Si-Al-OH) and hydroxyl groups on extra framework Al.[35] Within the wavenumber range, one can also obtain information about changes in the potency of the Brønsted acid site because of the addition of metal. There is a positive correlation between an increase in the total quantity of acid and an increase in the transmission intensity in the wavenumber range of around 2125 $cm^{-1}$. It can also be observed from the FTIR pattern that the loading of the ZSM-5 with Ni and Co did not lead to any significant change in transmission pattern in comparison with the parent ZSM-5 in the examined area. This supports the XRD data as there is no reduction in the above bands, indicating retention of crystallinity and functional groups after incorporation of the metal. This result is consistent with Dauda *et al.*,[39] Razavian and Fatemi,[40] Zhao *et al.*,[41] and Gurdeep Singh *et al.*[42]

### Scanning electron microscope, energy dispersive spectrometer and PSD

Figure 3(a)–(d) displays the image obtained from the scanning electron microscope, energy dispersive spectrometer (SEM-EDS) examination of the catalysts. The catalysts have a spherical structure, and the PSD is homogeneous across the entire particle density, including

© 2023 The Authors. *Biofuels, Bioproducts and Biorefining* published by Society of Industrial Chemistry and John Wiley & Sons Ltd.


19321031, 2024, 3, Downloaded from https://scijournals.onlinelibrary.wiley.com/doi/10.1002/bbb.2536 by South African Medical Research, Wiley Online Library on [27/08/2024]. See the Terms and Conditions (https://onlinelibrary.wiley.com/terms-and-conditions) on Wiley Online Library for rules of use; OA articles are governed by the applicable Creative Commons License

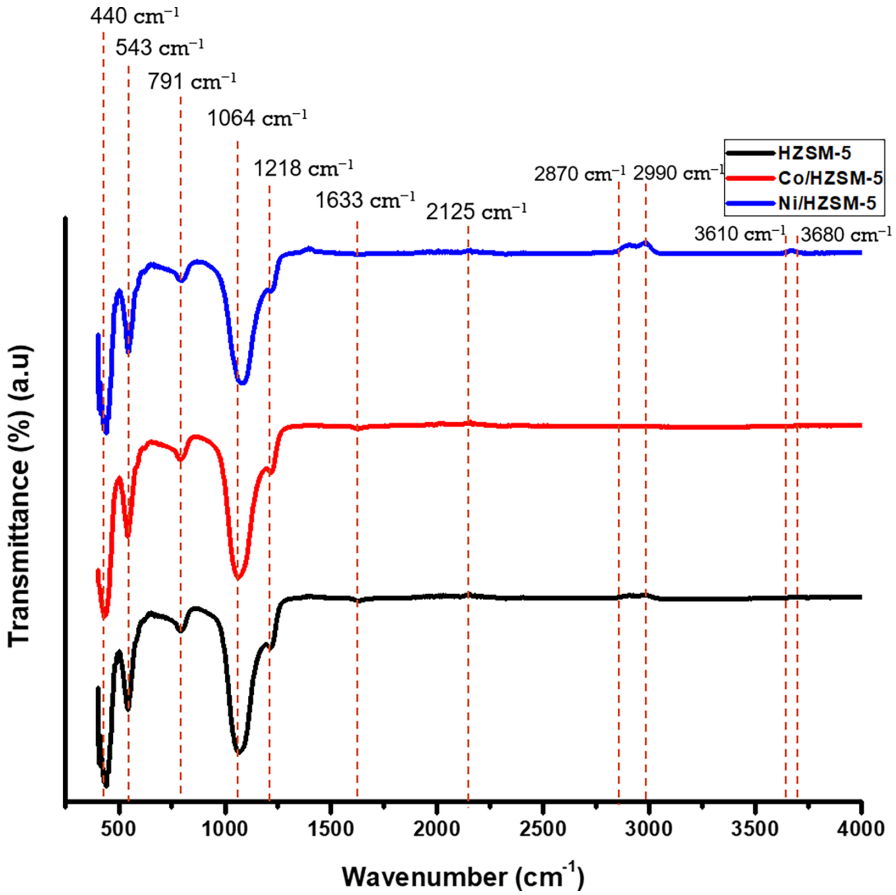


Figure 2. FTIR of parent and transition metal-doped HZSM-5.

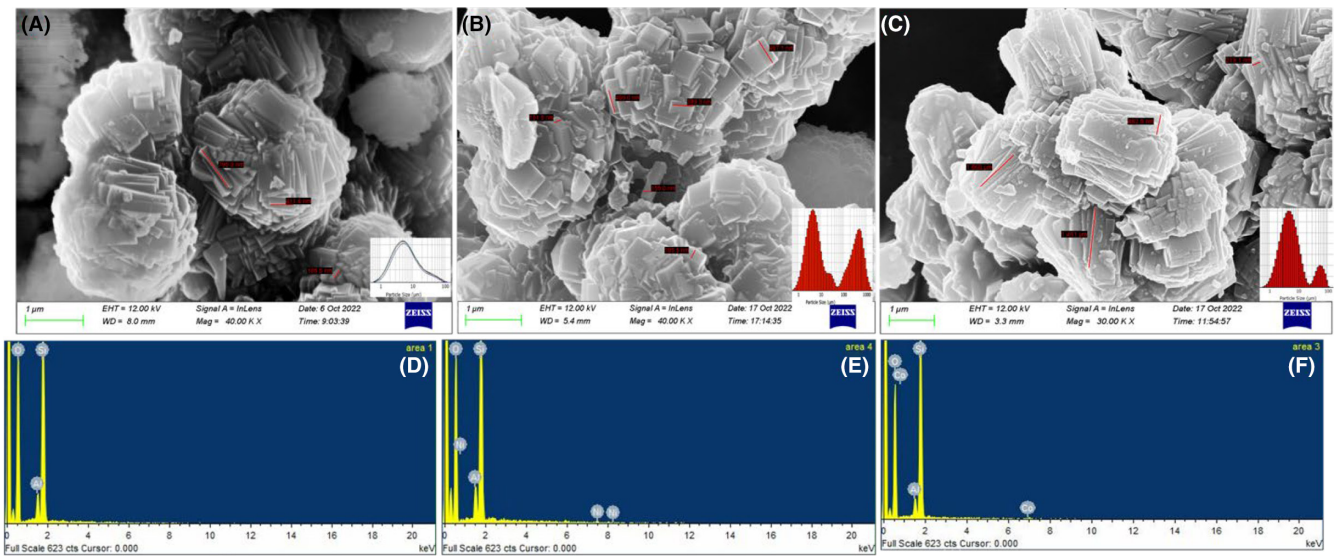


Figure 3. SEM images and EDS spectra of (a and d) HZSM-5 (b and e) Ni/HZSM-5 (c and f) Co/HZSM-5.

the smooth surface on the outside. On the ZSM-5 zeolite parent and modified catalysts, the MFI crystals have a homogeneous prismatic shape, the usual structure of MFI crystals. The micro-spherical aggregation of individual nanocrystals may be seen on the surface morphology of the parent catalyst and the modified catalyst. This kind of


© 2023 The Authors. *Biofuels, Bioproducts and Biorefining* published by Society of Industrial Chemistry and John Wiley & Sons Ltd.


19321031, 2024, 3, Downloaded from https://scijournals.onlinelibrary.wiley.com/doi/10.1002/bbb.2536 by South African Medical Research, Wiley Online Library on [27/08/2024]. See the Terms and Conditions (https://onlinelibrary.wiley.com/terms-and-conditions) on Wiley Online Library for rules of use; OA articles are governed by the applicable Creative Commons License

morphology results in a mesoporous structure, which, as per intra-crystal spaces, ultimately leads to an improvement in the diffusion of molecules within the structure of the catalyst. The morphology of ZSM-5 zeolites does not change following metal modification using the IWI synthesis approach;[43] nevertheless, the particle size of ZSM-5 zeolites was altered according to the PSD analysis. The particle size of the parent ZSM-5 (4.55 µm) increased by 0.19 and 1.78 µm with Co and Ni species incorporation, respectively. This indicates that incorporating metal species increased catalyst particle sizes, as nickel nanoparticles are larger than those of cobalt.[44,45] During the incipient wetness impregnation method, the Co- and Ni-metal species can diffuse into the zeolite's channels and pores and cause lattice expansion or contraction.[46] The charged metal species can also form oxides or clusters that can block the pore entrances partially and affect the effective size of the catalyst and other structural properties.[46–48]

## Textural properties

The textural characteristics of the catalysts are outlined in Table 1. The as-synthesized ZSM-5 support showed a significant surface area and a multi-porous volume, both beneficial for dispersing active metal species and preventing aggregation.[49] In comparison with catalysts from other studies, the synthesized ZSM-5 of the present study has a considerably specific surface area (397.5 $m^2 g^{-1}$). The introduction of a little quantity of transition metal species by the impregnation process resulted in changes to the BET surface area, pore volume, and pore diameter of those catalysts with respect to the parent ZSM-5 zeolite. Hence, a slight increase in mesopores was observed while the surface area and average pore diameter decreased with transition metal modification. The decrease in $S_{BET}$ is due to transition metals (Co, Fe, and Ni) species covering the surface of ZSM-5 and partly blocking zeolite channels. During the modification process with transition metals, there is a tendency to clog the pores of the zeolite channels with metal species, resulting in the synthesis of a metal-doped zeolite with a reduced surface area.[50] Consistent with this present study, Zheng *et al.*[34] noted that the specific surface area of the unmodified H-ZSM-5 was quite high (338.44 $m^2.g^{-1}$) in comparison with the specific surface area of the improved catalyst, which reduces, ranging from 293 $m^2 g^{-1}$ to 287 $m^2 g^{-1}$. The pore volume reduced but the pore size improved, although the change was insignificant. The deposition of metal species probably caused this at the catalyst opening or deep inside the channel, clogging the catalyst channel's interior and resulting in a decreased pore volume.[48] In addition, the blockage in the mesopores triggers a decrease in overall pore size, which shows that the metal ions were distributed uniformly on the ZSM-5 surface. These findings are comparable with those of Schultz and Elmore.[51]

Figure 4(a) illustrates the $N_2$ adsorption–desorption isotherms and the pore distribution of transition metal-doped ZSM-5 zeolites. The figure shows that the pure and the metal-doped ZSM-5 zeolites fabricated via the impregnation approach had comparable $N_2$ adsorption–desorption isotherms. The isotherms showed a hysteresis branch, which corresponds to a Langmuir isotherm (type IV) based on the IUPAC categorization, and the adsorption and desorption branches practically intersected at relatively low pressure, showing that the macro-mesoporous structures were well conserved after metal incorporation by the impregnation technique.[52–54] The adsorbed volume increased continuously with relative pressure. The improved adsorption in the pressure range of $0.4P/P_0$ has occurred from the adsorption of nitrogen within and intra-crystalline mesopores as a result of the aggregation of the nanocrystals. The hysteresis loop at increased pressure region ($P/P_0 = 0.85$) shows that large pores, from meso-to macro-pores, are observed for all catalysts studied. However, the larger hysteresis loop of 0.45 to 1 of relative partial pressure ($P/P_0$) in the HZSM-5 and Ni/HZSM-5 indicates that the sample contains a substantial mesoporous framework. It is important to note that the adsorbed amounts of HZSM-5 and Ni/HZSM-5 are almost an order of magnitude more than those of Co/HZSM-5, indicating that these catalysts (parent and Ni-doped) have a large surface area and a uniform pore structure. Hence, the BET surface area of HZSM-5 and Ni/HZSM-5 are 397.5 and 381.4 $m^2 g^{-1}$, respectively, while Co/HZSM-5 has the lowest surface area (362.6 $m^2 g^{-1}$) as per the results of $N_2$ absorption study. It can be inferred that, after incorporating the metal (Ni and Co) species framework, fewer mesoporous structures

**Table 1. Textural properties of pure and transition metal-modified HZSM-5.**

| Catalysts (Si/Al) | $S_{BET}$ ($m^2 g^{-1}$) | $S_{micro}$ ($m^2 g^{-1}$) | $V_{total}$ ($cm^3 g^{-1}$) | $V_{meso}$ ($cm^3 g^{-1}$) | $V_{macro}$ ($cm^3 g^{-1}$) | Avg pore dia. (nm) | Metal (wt%) | Other studies ($S_{BET}$ $m^2 g^{-1}$) |
|---|---|---|---|---|---|---|---|---|
| HZSM-5 (40) | 397.5 | 335.2 | 0.706 | 0.678 | 0.0285 | 2.224 | 0 | 342.9[57] 321.1[58] |
| Co/HZSM-5 | 362.6 | 312.4 | 0.461 | 0.456 | 0.0057 | 2.008 | 0.5 | 338.4[34] |
| Ni/HZSM-5 | 381.4 | 318.9 | 0.590 | 0.582 | 0.0083 | 2.024 | 0.5 | 338[59] |

© 2023 The Authors. *Biofuels, Bioproducts and Biorefining* published by Society of Industrial Chemistry and John Wiley & Sons Ltd.


19321031, 2024, 3, Downloaded from https://scijournals.onlinelibrary.wiley.com/doi/10.1002/bbb.2536 by South African Medical Research, Wiley Online Library on [27/08/2024]. See the Terms and Conditions (https://onlinelibrary.wiley.com/terms-and-conditions) on Wiley Online Library for rules of use; OA articles are governed by the applicable Creative Commons License

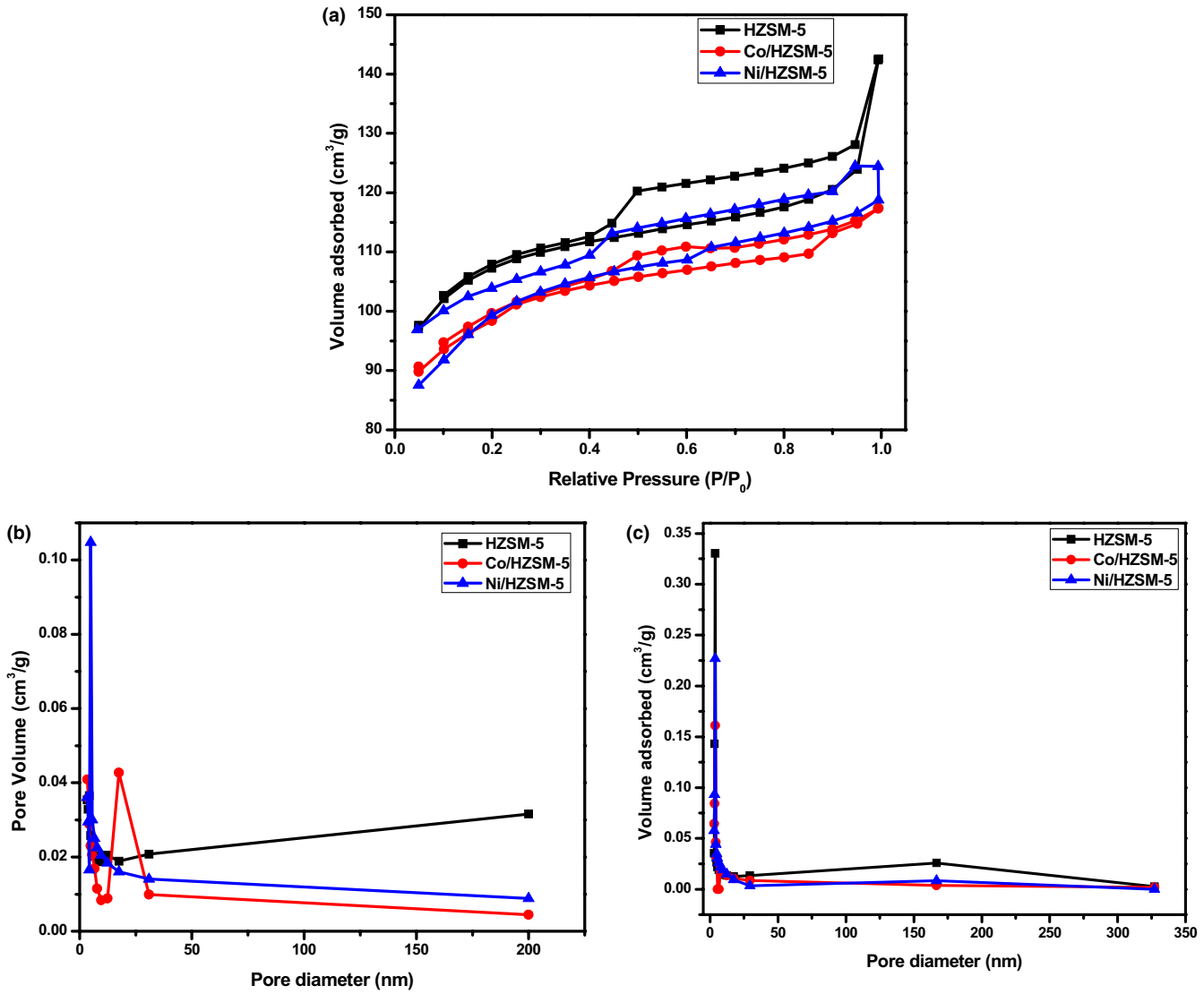


Figure 4. (a) $N_2$ adsorption–desorption isotherm; (b) BJH pore size distribution for adsorption, and (c) desorption of pure and transition metal-doped HZSM-5 catalysts.

were destroyed, and fewer macroporous structures were produced. This demonstrates a high degree of congruence with the pore pattern depicted in Fig. 4(b),(c), which agrees with the study by Wei *et al.*[54]

The corresponding pore-size distribution diagrams for adsorption and desorption are shown in Fig. 4(b),(c). These plots are deduced using the adsorption branch of the $N_2$ isotherm and the BJH method. The adsorption and desorption pore-size distribution diagram (Fig. 4(b),(c)) shows that HZSM-5 has a comparable pore size distribution with a hierarchical porous framework as its metal-doped counterpart (Ni- and Co-doped). However, the HZSM-5 exhibits a larger average pore diameter and total pore volume of 2.22 nm and 0.71 $cm^3 g^{-1}$ (in comparison with Co/HZSM-5) (2.01 nm and 0.46 $cm^3 g^{-1}$) and Ni/HZSM-5 (2.02 nm and 0.59 $cm^3 g^{-1}$). The hierarchical porous framework of these materials confirmed the porous hierarchy of the catalyst, where the porosity and structure of the porous framework encompass a range of pore sizes, from mesopores to macropores.[55] These unusual structures are attracting much interest due to their diversity, versatility and significant performance; moreover, they are utilized widely as an essential family of functional materials in catalysis. Furthermore, the larger mesopore size has the potential to accelerate mass transfer and reduce the limitation of internal diffusion, which in turn affects activity and product distribution. These results are consistent with those of Vitale *et al.*[47] and Zhang *et al.*[56]


© 2023 The Authors. *Biofuels, Bioproducts and Biorefining* published by Society of Industrial Chemistry and John Wiley & Sons Ltd.


19321031, 2024, 3, Downloaded from https://scijournals.onlinelibrary.wiley.com/doi/10.1002/bbb.2536 by South African Medical Research, Wiley Online Library on [27/08/2024]. See the Terms and Conditions (https://onlinelibrary.wiley.com/terms-and-conditions) on Wiley Online Library for rules of use; OA articles are governed by the applicable Creative Commons License

## $NH_3$-TPD results

Table 2 presents the $NH_3$-TPD results, which show the presence of three distinct peaks at different temperatures. The desorption of ammonia at low temperatures, corresponding to weak acid sites, increased from 0.95 mmol $g^{-1}$ $NH_3$ in HZSM-5 at 198 °C to 1.05 and 1.06 mmol $g^{-1}$ with the incorporation of Co and Ni metal species, respectively. The introduction of these metal species also caused a shift in the desorption temperatures, observed at 189 and 190 °C for the metal-doped samples. The desorption peaks at medium temperatures, known as moderately strong acid sites, showed a slight decrease with the addition of Co and Ni. The $NH_3$ desorption reduced to 0.69 and 0.68 mmol $g^{-1}$ at 425 and 435 °C, respectively, in comparison with HZSM-5, which recorded 0.74 mmol $g^{-1}$ at 419 °C. In contrast, a significant reduction in strong acid sites, specifically Brønsted acid sites, was observed. The amount of desorbed ammonia decreased from 0.024 mmol $g^{-1}$ at 686 °C in HZSM-5 to 0.015 and 0.014 mmol $g^{-1}$ at 667 and 688 °C, respectively. During the dry impregnation technique, it is important to note that some of the acidic protons responsible for the Brønsted acidity in the crystalline zeolite ZSM-5 may have undergone ion exchange with Co or Ni ions. The formation of metal oxides, which can function as Lewis or weak acid sites, also contributed to the significant reduction in Brønsted acid sites. The formation of these oxides may therefore reduce the availability of strong acid sites for $NH_3$ adsorption, as the metal hydroxides or metal oxides occupy the sites of strong acidity or dehydroxylation.[60]

## Catalytic performance

The catalytic activity of the catalysts was studied, focusing on their selectivity to various hydrocarbons (HCs). The catalytic activity of the catalysts was evaluated at different WHSVs (5 h and 12 $h^{-1}$) and temperatures (350–400 °C). For all conversions at different operating conditions, ethanol conversion greater than 98% and different product distributions were observed (Fig. 5). This is consistent with other studies,[61–64] as ethanol conversion rates close to 100% were obtained for all reactions at similar reaction temperatures. Both before and after doping with transition metals, the products of ZSM-5 contain a variety of hydrocarbons with disparities in distribution. All catalysts exhibited a range of gaseous and liquid HCs product distributions, including $C_1$-$C_4$, $C_5$-$C_8$, $C_9$-$C_{12}$, $C_{12}$+, and aromatics. At 5 $h^{-1}$ and 350 °C, the product distribution showed significant selectivity for gaseous HCs ($C_1$-$C_4$), with the unmodified catalyst exhibiting the highest gaseous product (85.2%) compared to the metal-modified catalysts with 45.5% and 66.5% for Co/HZSM-5 and Ni/HZSM-5, respectively (Fig. 5(a)). The selectivity of the gaseous product at these operating conditions may be attributed to the WHSV of 5 $h^{-1}$, a low WHSV (in comparison with 12 $h^{-1}$), which favors prolongation of the reaction time and a tendency to side reactions such as cracking of heavier HCs into lighter fractions. Co- and Ni-doped catalysts showed higher selectivity for liquid HCs than the parent catalyst. Among the catalysts evaluated at 5 $h^{-1}$ and 350 °C, Co/HZSM-5 exhibited the highest $C_{12}$+ selectivity (40.7%), while Ni/HZSM-5 favored benzene aromatic products with 2.2% selectivity. Moreover, the unmodified catalysts exhibited the lowest liquid HC fractions, and no aromatic products were generated. Previous research found that ethanol feed produced less than 5% aromatics and some fractions of lightweight HCs.[65]

In contrast to the results at 5 $h^{-1}$, the catalyst test at 12 $h^{-1}$ and the same temperature of 350 °C showed higher selectivity for liquid hydrocarbon and better wider product distribution than 5 $h^{-1}$ WHSV. Ni/ZSM-5 produced more $C_5$-$C_8$ (48.4%) and benzene (4.9%) than Co/HZSM-5 (29.8% and 1.1%) and unmodified catalysts, which had the lowest values of 28.6% and 1.0%, respectively (Fig. 5(b)). However, HZSM-5, Co/HZSM-5 and Ni/HSM-5 showed the highest selectivity for $C_{12}$+, $C_9$-$C_{12}$ and $C_5$-$C_8$ HCs, respectively. As-synthesized HZSM-5 exhibited the highest $C_{12}$+ selectivity (52.1%) but a decrease in this HC fraction was observed for metal-doped catalysts, resulting in increased $C_9$-$C_{12}$ (16.2%) and benzene (4.9%) production for Co/HZSM-5 and Ni/HZSM-5, respectively. This operating condition favored the production of condensable hydrocarbons (large molecules), mainly $C_5$-$C_8$ and $C_{12}$+. Previous studies have shown that the complete dehydration of ethanol, leading to the formation of gaseous products ($C_1$-$C_4$ hydrocarbons), occurs at temperatures

**Table 2. $NH_3$-TPD results of pure and metal-doped catalysts.**

| Catalysts | Acidity conc. (mmol $NH_3$ $g^{-1}$) | | | Total acidity |
|---|---|---|---|---|
| | Weak (T = 100–300 °C) | Moderate (T = 300–500 °C) | Strong (T = 500–700 °C) | |
| HZSM-5 | 0.95 | 0.74 | 0.024 | 1.714 |
| Co/HZSM-5 | 1.05 | 0.69 | 0.015 | 1.755 |
| Ni/HZSM-5 | 1.06 | 0.68 | 0.014 | 1.764 |

© 2023 The Authors. *Biofuels, Bioproducts and Biorefining* published by Society of Industrial Chemistry and John Wiley & Sons Ltd.


19321031, 2024, 3, Downloaded from https://scijournals.onlinelibrary.wiley.com/doi/10.1002/bbb.2536 by South African Medical Research, Wiley Online Library on [27/08/2024]. See the Terms and Conditions (https://onlinelibrary.wiley.com/terms-and-conditions) on Wiley Online Library for rules of use; OA articles are governed by the applicable Creative Commons License

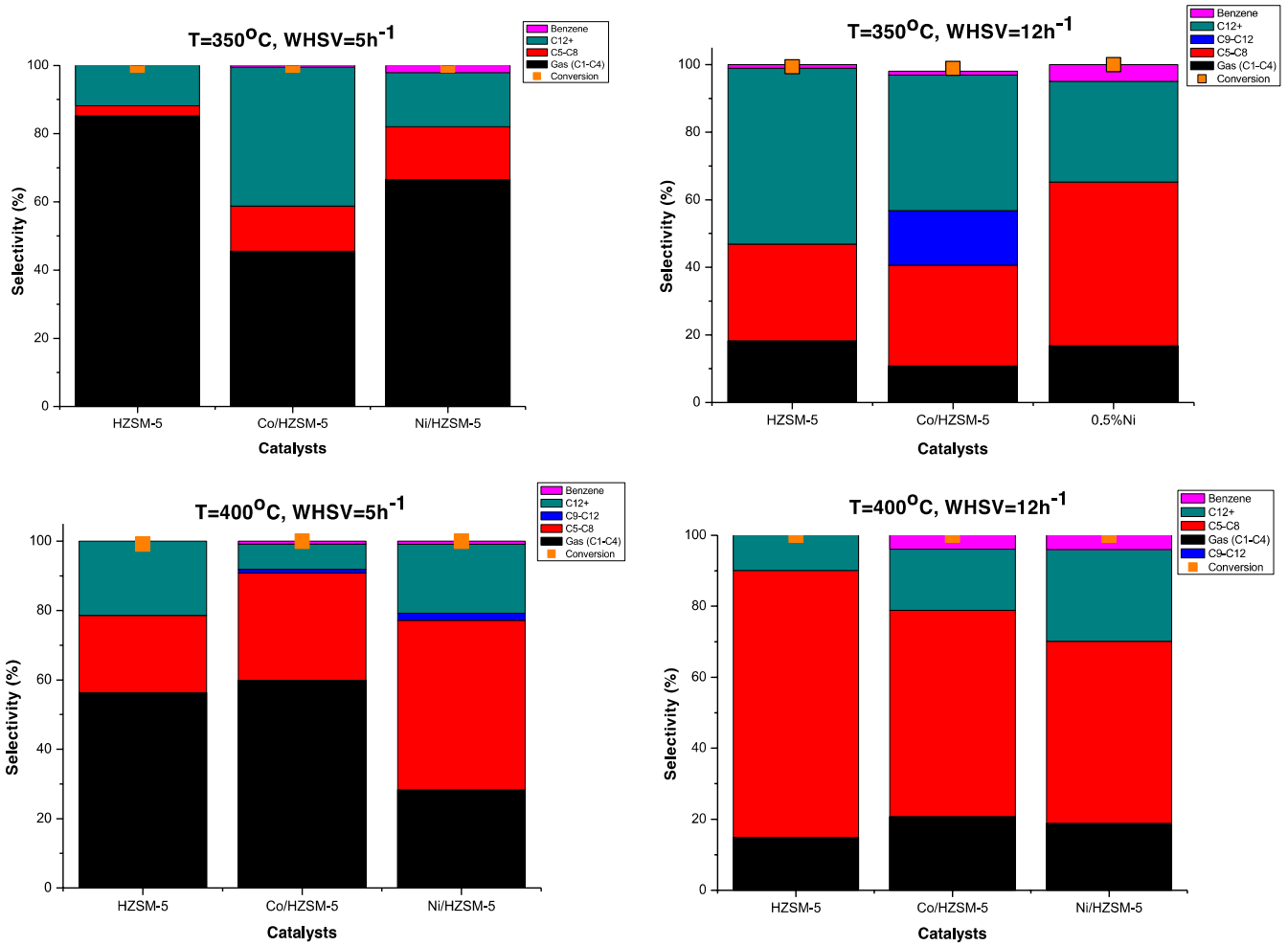


Figure 5. Hydrocarbon product distribution for parent and transition metal-doped HZSM-5 at T = 350 and 400 °C and WHSV = 5 and 12 $h^{-1}$.

between 200 °C and 300 °C,[29,66–69] while the aromatization of ethanol, leading to the formation of liquid products, only occurs at temperatures of 350 °C and above.[7,13,65,70] This further explains the rise in liquid HCs because ethanol oligomerizations were more favorable at temperatures starting at 350 °C.

Increasing the operating temperature to 400 °C decreased gaseous HC selectivity at all of the WHSVs studied (Fig. 5(c)). Ethanol conversion over HZSM-5 and metal-doped catalysts showed that all investigated catalysts achieved ethanol conversion greater than 98% at this operating parameter. At 5 $h^{-1}$ and T = 400 °C, Co- and Ni-doped catalysts produced more $C_5$-$C_8$ (30.9 and 48.8%) and lower amounts of $C_9$-$C_{12}$ (1.1 and 2.1%) and benzene (0.85 and 0.92%) aromatics, compared to unmodified HZSM-5, which favored gaseous (56.5%) and $C_{12}$+ (21.4%) HCs. However, at 12 $h^{-1}$ and 400 °C, the product contained more liquid than gases, which is due to the reaction parameters used (Fig. 5(d)). The WHSV, the factor that regulates the contact time with the catalyst, can be used to explain this; for example, a higher WHSV indicates a higher flow rate and, thus a lower residence time with the catalyst. The less interaction the hydrocarbon has with the catalyst, the fewer secondary reactions occur, leading to higher selectivity and production of heavier HCs.[71,72] This operating condition promotes the production of $C_8$-$C_{12}$, with the unmodified HZSM-5 having a reasonable selectivity of 75.1%. Compared with the unmodified HZSM-5, the slightly lower selectivity of the $C_5$-$C_{12}$ HC fractions observed with the metal-doped catalysts Co/HZSM-5 and Ni/HZSM-5 can be due to the presence of metal species in the catalysts, leading to a shift in $C_5$-$C_{12}$ selectivity toward other HC fractions. Consequently, for Co- and Ni-doped catalysts, an increase in the selectivity of the HC fractions $C_{12}$+ (17.2 and 25.9%) and benzene (3.8 and 3.9%) was observed in the product distribution. These values correspond to an increase in these HC fractions compared to 5 $h^{-1}$.[71,72] We suggest that the


© 2023 The Authors. *Biofuels, Bioproducts and Biorefining* published by Society of Industrial Chemistry and John Wiley & Sons Ltd.


19321031, 2024, 3, Downloaded from https://scijournals.onlinelibrary.wiley.com/doi/10.1002/bbb.2536 by South African Medical Research, Wiley Online Library on [27/08/2024]. See the Terms and Conditions (https://onlinelibrary.wiley.com/terms-and-conditions) on Wiley Online Library for rules of use; OA articles are governed by the applicable Creative Commons License

promoters lead to oligomerization and possible aromatization reactions.

Changing the temperature on catalytic activity revealed that an increase in temperature from 350 °C to 400 °C at constant WHSV ($5\,h^{-1}$) resulted in a shift in selectivity from gaseous HCs to liquid HCs, which favored more of $C_5$-$C_8$ hydrocarbons. In addition, the metal-doped catalyst produced more $C_9$-$C_{12}$ and small amounts of aromatics in contrast to non-modified catalysts. However, a WHSV of $12\,h^{-1}$ and an increase in reaction temperature led to a rise in the production of $C_9$-$C_{12}$ and benzene, resulting in a decrease in $C_{12}$+ selectivity at 400 °C. Benzene and more liquid product distribution were observed with the metal-doped catalysts.[7,13,65,70] Figure 6 shows the phase selectivity of the different catalysts studied at different operating conditions. It was found that a lower WHSV ($5\,h^{-1}$) favored gaseous HC while increasing the WHSV to $12\,h^{-1}$ shifted the selectivity toward the liquid HC fractions at all temperatures studied (Fig. 6). However, at WHSV of $5\,h^{-1}$, more liquid HC fractions are produced at 400 °C than at 350 °C operating temperature. In general, the unmodified catalyst showed the lowest selectivity for liquid hydrocarbon, while Co- and Ni-doped catalysts showed the highest selectivity (>79%) at a WHSV of $12\,h^{-1}$ and $5\,h^{-1}$ favors gaseous product. This indicates that the metal-doped catalyst favors the production of liquid HCs and improves product distribution.[59]

It has been suggested that ethanol is converted to liquid, or $C_5$+ HCs, using a dual-cycle HC pool that first dehydrates the ethanol before aromatization. The process known as the ethanol hydrocarbon pool (HCP) begins with ethylene synthesis, which is then converted to BTX by the intrinsic framework of the HZSM-5 pore.[14,69] Due to the enormous size of some aromatic and $C_9$+ HCs concerning the pore size/volume capacity, the ethanol HCP approach can only produce a small amount of these HCs.[14] However, more $C_9$+ HCs are generated because of the multiporous structure of the catalysts used in this study. This can be explained by the fact that the pore space is large enough to contain a greater number of intermediate HCs and BTX for single-stage transformation into $C_9$+ HCs. The wider pores in the doped ZSM-5 also enhance the liquid hydrocarbon yield (LHY) because they allow a considerable proportion of active metal to be incorporated into the zeolite pores.[59] Heavyweight $C_9$+ HCs can form on the exterior surface of ZSM-5 or within its pores due to the $C_7$/$C_8$ alkylation with $C_1$/$C_2$ HCs.[59] Any chains that are too long to pass via the pore mouth will either have to break into smaller molecules capable of escaping through the zeolite's micro/mesopores, or they will need to disassemble and deposit carbon on the walls, which will either obstruct the adsorption or clog the micropores. Due to the high surface area and combined mesopores and macropores in HZSM-5 and modified-HZSM-5 framework and the operating conditions employed, performing successive ethanol dehydration, aromatization, and alkylation was feasible, which enhanced the production of long-chain ($C_5$+) HCs. This combination also helped minimize the trapping of heavy $C_8$+ HCs, which would have otherwise cracked into smaller molecules that could escape or pyrolyze into coke, interfering with the catalytic activity inside the pores.[59] Hence, the findings of this investigation demonstrated that the catalyst could sustain a stable synthesis of $C_5$+ HCs. Due to decreased support crystallinity and metal–support contact, the specificity to liquid HCs with more than eight carbon atoms (mainly C9-C12) declined dramatically in some instances. However, by preserving crystallinity while enhancing pore capacity, post-treatment of ZSM-5 with transition metal-doping (Ni and Co) enhanced both liquid hydrocarbon yields (LHYs) and selectivity to $C_5$+ HCs. By facilitating metal mobility into ZSM-5 channels and promoting strong metal–support contacts, increasing pores *via* metal doping allowed

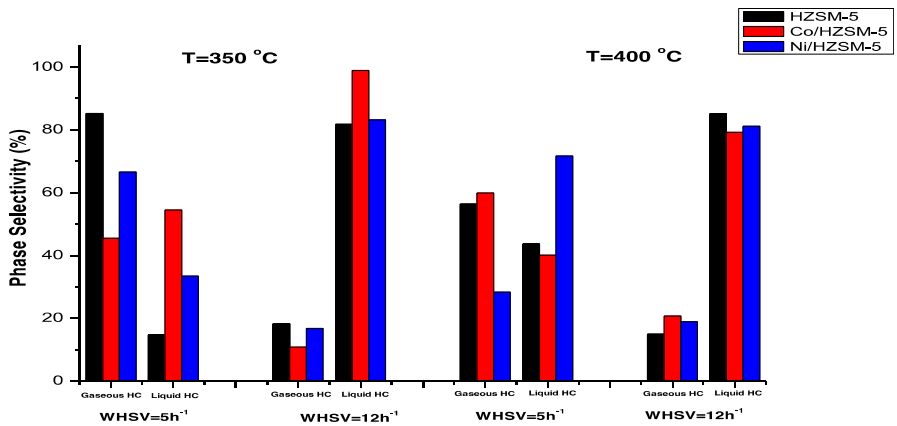


Figure 6. Hydrocarbon gaseous and liquid phase selectivity at varying operating conditions.

© 2023 The Authors. *Biofuels, Bioproducts and Biorefining* published by Society of Industrial Chemistry and John Wiley & Sons Ltd.


19321031, 2024, 3, Downloaded from https://scijournals.onlinelibrary.wiley.com/doi/10.1002/bbb.2536 by South African Medical Research, Wiley Online Library on [27/08/2024]. See the Terms and Conditions (https://onlinelibrary.wiley.com/terms-and-conditions) on Wiley Online Library for rules of use; OA articles are governed by the applicable Creative Commons License

19321031, 2024, 3, Downloaded from https://scijournals.onlinelibrary.wiley.com/doi/10.1002/bbb.2536 by South African Medical Research, Wiley Online Library on [27/08/2024]. See the Terms and Conditions (https://onlinelibrary.wiley.com/terms-and-conditions) on Wiley Online Library for rules of use; OA articles are governed by the applicable Creative Commons License

for a substantial increase in $C_5$+ specificity from ethanol dehydration, aromatization, and alkylation. The innate pore framework of ZSM-5 and metal-doped ZSM-5 therefore played a crucial role in regulating and promoting LHYs. This is consistent with Seemala and Wyman.[59]

The typical pathway for transforming primary alcohols, like ethanol, involves intermolecular dehydration, leading to the formation of ethylene and diethyl ether (DEE) through a concerted mechanism (a pathway involving a single transition state and no intermediate). This pathway is preferred due to the high energy barrier associated with the formation of a primary carbocation intermediate. It has also been suggested that DEE can undergo cracking, generating ethylene, which can then participate in subsequent reactions, creating an alternative reaction pathway for ETH conversion. The cracking of DEE, as a secondary carbocation intermediate, can occur through acid-catalyzed or radical mechanisms depending on the reaction conditions and catalyst properties. Ethylene produced from the dehydration and cracking steps can further undergo dehydrogenation reactions to form ethyl radicals. These ethyl radicals are highly reactive intermediates that can participate in various secondary reaction pathways. In the dehydrogenation step, ethyl radicals react with adsorbed hydrocarbon species on the ZSM-5 catalyst, forming a carbocation. Aromatization reactions involve the cyclization of carbocation formed initially, producing aromatic hydrocarbons such as benzene. These reactions occur through a series of rearrangement reactions of the carbocation intermediates. Besides aromatization, ZSM-5 catalysts also facilitate the formation of long-chain hydrocarbons, $C_5$+, through oligomerization reactions. These HCs are typically formed through secondary carbocation reactions or additional transformations of the intermediates generated during aromatization.[6,73–75] In the case of the metal-doped ZSM-5, the enhanced performance of the doped catalyst can be attributed to the presence of metal species that actively participate in the HC reaction. Compared to the unmodified catalysts, the metal species ($Co^{2+}$ and $Ni^{2+}$) present in the metal-doped catalysts play a crucial role in promoting the formation of intermediates. These intermediates act as Lewis acid sites during the HC reaction. The Lewis acid sites facilitated by the metal species promote the dehydration of ethanol, leading to increased ethylene production. The availability of more ethylene promotes secondary reactions, resulting in broader product distribution.[6] However, metal doping can increase the likelihood of coke deposition and subsequent catalyst deactivation. As a result, the unmodified catalyst exhibits greater stability than the metal-doped catalyst.

The framework structure, pore-size distribution, textural characteristics, and acidity of the ZSM-5 catalyst all play essential roles in determining the low alcohol conversion performance.[76,77] The distributions of the products were affected by the properties of the catalysts because, following metal incorporation, the attributes of the HZSM-5 support were altered. The acidity and surface area of the catalyst were among the most critical factors that determined its catalytic performance.[78] Recent research has shown that acidity plays an integral part in the design of low-alcohol conversion catalysts.[79] These findings have highlighted the requirement for optimal strength and concentration of acid sites to achieve an adequate product distribution over the catalyst. Thus, metal impregnation alters catalyst acidity, increases catalytic activity, and produces a very effective catalyst for the reaction involving low alcohol. The impregnation also minimizes severe acidity and reduces undesired secondary processes.[58] It was discovered that the introduction of transition metals increased the number of Lewis acid sites in the original HZSM-5.[78] In contrast to Brønsted acid sites, this form of the acid site can decrease significantly the secondary cracking of liquid into gaseous HCs. As a result, the synergistic action of metals with HZSM-5 led to improved product distribution efficiency compared to the stand-alone original HZSM-5 catalyst. This explained the high liquid yield in the present study using metal-doped ZSM-5. However, the low yield of benzene observed in the current study can be attributed to the specific operating parameters employed, which may not favor high benzene selectivity. This finding is consistent with previous studies,[13,65,80] which reported similar benzene yields. A study by Calsavara *et al.*[81] also highlighted a predominance of xylene and toluene aromatics compared to benzene during ETH conversion at 400 °C.

Notably, fuel-range hydrocarbons account for a more significant proportion of the liquid HCs produced by all catalysts considered in this work. The relative abundance of heavy HCs in the liquid content of the HZSM-5 catalysts experienced a modest increase after the metal-modified catalyst was employed. This can be attributed to the appropriate environment provided by transition metal species incorporated on HZSM-5 for the oligomerization reaction of shorter-chain alkenes. Consequently, the bifunctional properties of the metal sites and acid sites ultimately lead to the generation of heavier HCs.[82] Moreover, these metals (Ni and Co) modified zeolites showed a notable affinity for oligomerization in this study. Metal oxide is frequently utilized to increase the yields of liquid HC and aromatics. It is mostly studied in catalytic cracking reactions: metal oxide introduces extra functionality when dehydrogenation and aromatization occur, and oligomerization, cyclization,


© 2023 The Authors. *Biofuels, Bioproducts and Biorefining* published by Society of Industrial Chemistry and John Wiley & Sons Ltd.

dealkylation, transalkylation, and isomerization occur on the acid site. In most instances, this is carried out at increased temperatures.[79] As more $C_1$-$C_4$ HCs are detected at lower WHSVs, they can be termed the reactants for the formation of $C_5$+ HCs. The oligomerization of olefins can result in the synthesis of heavier HCs. These HCs can further undergo cracking or hydrogen transfer process depending on factors (including catalyst promoters and operating conditions) to produce target HC products.

## Conclusion

The transformation of ethanol to fuel-range HCs was studied on metal-doped synthesized HZSM-5 (Si/Al = 40). HZSM-5 was modified with transition metals (Co and Ni) at 0.5 wt%. A combined catalytic test and thorough catalyst study (XRD, FTIR, SEM, EDS, PSD, BET and $N_2$ adsorption) identified various influences of metal doping on HZSM-5 catalyst and activity. Ethanol conversion of more than 98% was achieved with all catalysts studied. The transition metal-doped catalysts, Ni/HZSM-5 and Co/HZSM-5, showed wider product distribution and selectivity for liquid C5+ HCs at a WHSV of 12 $h^{-1}$. The unmodified catalyst exhibited the highest selectivity for gaseous ($C_1$-$C_4$) HCs (85.2%) at 5 $h^{-1}$ and 350 °C, but Co/HZSM-5 was more selective for liquid HCs with 58.16, 16.17, 40.7 and 3.9%, while Ni/HZSM-5 exhibited 51.25, 2.0, 29.8 and 5% for $C_5$-$C_8$, $C_9$-$C_{12}$ and $C_{12}$+ and benzene, respectively. The study showed that incorporating metal into HZSM-5 improved the production of liquid HCs and benzene selectivity. The synthesized catalysts can therefore be viable for upgrading ethanol into fuel-range hydrocarbons.

## Acknowledgements

This work was supported financially by an international collaborative project (BRICS2019-040) under the BRICS STI Framework Programme with government funding organizations of South Africa (NRF, BRIC190321424123), Brazil (CNPq, 402 849/2019-1), Russia (RFBR, 19-58-80 016), India (DST, CRG/2018/004610, DST/TDT/TDP-011/2017), and China (MOST, 2018YFE0183600).

## References

1. Centi G, Lanzafame P and Perathoner S, Analysis of the alternative routes in the catalytic transformation of lignocellulosic materials. *Catal Today* **167**(1):14–30 (2011). https://doi.org/10.1016/j.cattod.2010.10.099.
2. Anekwe IMS, Khotseng L and Isa YM, The place of biofuel in sustainable living; prospects and challenges, in *Reference Module in Earth Systems and Environmental Sciences*. Elsevier, Amsterdam, Netherlands, (2021).
3. Abdellatief TM, Ershov MA, Kapustin VM, Abdelkareem MA, Kamil M and Olabi A, Recent trends for introducing promising fuel components to enhance the anti-knock quality of gasoline: a systematic review. *Fuel* **291**:120112 (2021).
4. Gonçalves A *et al*., Towards the development of syngas/biomethane electrolytic production, using liquefied biomass and heterogeneous catalyst. *Energies* **12**(19):3787 (2019).
5. Surisetty VR, Dalai AK and Kozinski J, Alcohols as alternative fuels: an overview. *Appl Catal Gen* **404**(1):1–11 (2011). https://doi.org/10.1016/j.apcata.2011.07.021.
6. Sun J and Wang Y, Recent advances in catalytic conversion of ethanol to chemicals. *ACS Catal* **4**(4):1078–1090 (2014). https://doi.org/10.1021/cs4011343.
7. Van der Borght K, Galvita VV and Marin GB, Reprint of "ethanol to higher hydrocarbons over Ni, Ga, Fe-modified ZSM-5: effect of metal content". *Appl Catal Gen* **504**:621–630 (2015). https://doi.org/10.1016/j.apcata.2015.06.034.
8. Derouane EG *et al*., Elucidation of the mechanism of conversion of methanol and ethanol to hydrocarbons on a new type of synthetic zeolite. *J Catal* **53**(1):40–55 (1978). https://doi.org/10.1016/0021-9517(78)90006-4.
9. Nguyen TM and Le Van Mao R, Conversion of ethanol in aqueous solution over ZSM-5 zeolites: study of the reaction network. *Appl Catal* **58**(1):119–129 (1990). https://doi.org/10.1016/S0166-9834(00)82282-4.
10. Aguayo AT, Gayubo AG, Tarrío AM, Atutxa A and Bilbao J, Study of operating variables in the transformation of aqueous ethanol into hydrocarbons on an HZSM-5 zeolite. *J Chem Technol Biotechnol* **77**(2):211–216 (2002). https://doi.org/10.1002/jctb.540.
11. Tret'yakov VF, Makarfi YI, Tret'yakov KV, Frantsuzova NA and Talyshinskii RM, The catalytic conversion of bioethanol to hydrocarbon fuel: a review and study. *Catal Ind* **2**(4):402–420 (2010). https://doi.org/10.1134/S2070050410040161.
12. Madeira FF, Gnep NS, Magnoux P, Maury S and Cadran N, Ethanol transformation over HFAU, HBEA and HMFI zeolites presenting similar Brønsted acidity. *Appl Catal Gen* **367**(1):39–46 (2009). https://doi.org/10.1016/j.apcata.2009.07.033.
13. Inaba M, Murata K, Saito M and Takahara I, Ethanol conversion to aromatic hydrocarbons over several zeolite catalysts. *React kinet catal lett* **88**(1):135–141 (2006). https://doi.org/10.1007/s11144-006-0120-5.
14. Johansson R, Hruby S, Rass-Hansen J and Christensen C, The hydrocarbon Pool in ethanol-to-gasoline over HZSM-5 catalysts. *Catal Lett* **127**:1–6 (2009). https://doi.org/10.1007/s10562-008-9711-2.
15. Gayubo AG, Alonso A, Valle B, Aguayo AT, Olazar M and Bilbao J, Kinetic modelling for the transformation of bioethanol into olefins on a hydrothermally stable Ni–HZSM-5 catalyst considering the deactivation by coke. *Chem Eng J* **167**(1):262–277 (2011). https://doi.org/10.1016/j.cej.2010.12.058.
16. Madeira FF, Gnep NS, Magnoux P, Vezin H, Maury S and Cadran N, Mechanistic insights on the ethanol transformation into hydrocarbons over HZSM-5 zeolite. *Chem Eng J* **161**(3):403–408 (2010). https://doi.org/10.1016/j.cej.2010.01.026.
17. Rahimi N and Karimzadeh R, Catalytic cracking of hydrocarbons over modified ZSM-5 zeolites to produce light olefins: a review. *Appl Catal Gen* **398**(1):1–17 (2011). https://doi.org/10.1016/j.apcata.2011.03.009.
18. Isa YM, Mohammed UA, Musamali R and Anekwe IM, Water treated promoted catalysts for the conversion of ethanol to hydrocarbons, in *Sustainable Energy-Water-*

© 2023 The Authors. *Biofuels, Bioproducts and Biorefining* published by Society of Industrial Chemistry and John Wiley & Sons Ltd.


19321031, 2024, 3, Downloaded from https://scijournals.onlinelibrary.wiley.com/doi/10.1002/bbb.2536 by South African Medical Research, Wiley Online Library on [27/08/2024]. See the Terms and Conditions (https://onlinelibrary.wiley.com/terms-and-conditions) on Wiley Online Library for rules of use; OA articles are governed by the applicable Creative Commons License

*Environment Nexus in Deserts*, ed. by Cham E, Heggy VB and Vermeersch M. Springer International Publishing, Cham, Switzerland, pp. 385–392 (2022).
19. Thybaut JW and Marin GB, Kinetic modeling of the conversion of complex hydrocarbon feedstocks by acid catalysts. *Chem Eng Technol* **26**(4):509–514 (2003). https://doi.org/10.1002/ceat.200390076.
20. Zakaria ZY, Linnekoski J and Amin NAS, Catalyst screening for conversion of glycerol to light olefins. *Chem Eng J* **207-208**:803–813 (2012). https://doi.org/10.1016/j.cej.2012.07.072.
21. Hagen A and Roessner F, Ethane to aromatic hydrocarbons: past, present, future. *Catal Rev Sci Eng* **42**(4):403–437 (2000). https://doi.org/10.1081/CR-100101952.
22. Viswanadham N, Muralidhar G and Rao TSRP, Cracking and aromatization properties of some metal modified ZSM-5 catalysts for light alkane conversions. *J Mol Catal A Chem* **223**(1):269–274 (2004). https://doi.org/10.1016/j.molcata.2003.11.045.
23. Heveling J, Nicolaides CP and Scurrell MS, Catalysts and conditions for the highly efficient, selective and stable heterogeneous oligomerisation of ethylene. *Appl Catal Gen* **173**(1):1–9 (1998). https://doi.org/10.1016/S0926-860X(98)00147-1.
24. Lu J, Zhao Z, Xu C, Zhang P and Duan A, FeHZSM-5 molecular sieves – highly active catalysts for catalytic cracking of isobutane to produce ethylene and propylene. *Catal Commun* **7**(4):199–203 (2006). https://doi.org/10.1016/j.catcom.2005.10.011.
25. Gayubo AG, Alonso A, Valle B, Aguayo AT, Olazar M and Bilbao J, Hydrothermal stability of HZSM-5 catalysts modified with Ni for the transformation of bioethanol into hydrocarbons. *Fuel* **89**(11):3365–3372 (2010). https://doi.org/10.1016/j.fuel.2010.03.002.
26. Inaba M, Murata K, Saito M and Takahara I, Production of olefins from ethanol by Fe-supported zeolite catalysts. *Green Chem* **9**(6):638–646 (2007).
27. Machado NRCF, Calsavara V, Astrath NGC, Matsuda CK, Paesano A and Baesso ML, Obtaining hydrocarbons from ethanol over iron-modified ZSM-5 zeolites. *Fuel* **84**(16):2064–2070 (2005). https://doi.org/10.1016/j.fuel.2005.05.001.
28. Saha S and Sivasanker S, Influence of Zn-and Ga-doping on the conversion of ethanol to hydrocarbons over ZSM-5. *Catal Lett* **15**(4):413–418 (1992).
29. Barthos R, Széchenyi A and Solymosi F, Decomposition and aromatization of ethanol on ZSM-based catalysts. *J Phys Chem B* **110**(43):21816–21825 (2006). https://doi.org/10.1021/jp063522v.
30. Goto D, Harada Y, Furumoto Y, Takahashi A, Fujitani T, Oumi Y *et al*., Conversion of ethanol to propylene over HZSM-5 type zeolites containing alkaline earth metals. *Appl Catal Gen* **383**(1):89–95 (2010). https://doi.org/10.1016/j.apcata.2010.05.032.
31. Song Z, Takahashi A, Mimura N and Fujitani T, Production of propylene from ethanol over ZSM-5 zeolites. *Catal Lett* **131**(3):364–369 (2009).
32. Sun Y, Ma T, Zhang L, Song Y, Shang Y, Zhai Y *et al*., "the influence of zoned Al distribution of ZSM-5 zeolite on the reactivity of hexane cracking," *molecular. Catalysis* **484**:110770 (2020). https://doi.org/10.1016/j.mcat.2020.110770.
33. Bayat A and Sadrameli S, Production of renewable aromatic hydrocarbons via conversion of canola oil methyl ester (CME) over zinc promoted HZSM-5 catalysts. *Renew Energy* **106**:62–67 (2017).
34. Zheng Y, Wang F, Yang X, Huang Y, Liu C, Zheng Z *et al*., Study on aromatics production via the catalytic pyrolysis vapor upgrading of biomass using metal-loaded modified H-ZSM-5. *J Anal Appl Pyrolysis* **126**:169–179 (2017).
35. Li X, Alwakwak A-A, Rezaei F and Rownaghi AA, Synthesis of Cr, Cu, Ni, and Y-doped 3D-printed ZSM-5 monoliths and their catalytic performance for n-hexane cracking. *ACS Appl Energy Mater* **1**(6):2740–2748 (2018). https://doi.org/10.1021/acsaem.8b00412.
36. Cheng Y, Wang L-J, Li J-S, Yang Y-C and Sun X-Y, Preparation and characterization of nanosized ZSM-5 zeolites in the absence of organic template. *Mater Lett* **59**(27):3427–3430 (2005).
37. Allahyari S, Haghighi M, Ebadi A and Hosseinzadeh S, Ultrasound assisted co-precipitation of nanostructured CuO–ZnO–Al2O3 over HZSM-5: effect of precursor and irradiation power on nanocatalyst properties and catalytic performance for direct syngas to DME. *Ultrason Sonochem* **21**(2):663–673 (2014).
38. Ali M, Brisdon B and Thomas W, Synthesis, characterization and catalytic activity of ZSM-5 zeolites having variable silicon-to-aluminum ratios. *Appl Catal Gen* **252**(1):149–162 (2003).
39. Dauda IB, Yusuf M, Gbadamasi S, Bello M, Atta AY, Aderemi BO *et al*., Highly selective hierarchical ZnO/ZSM-5 catalysts for propane aromatization. *ACS omega* **5**(6):2725–2733 (2020).
40. Razavian M and Fatemi S, Synthesis and evaluation of seed-directed hierarchical ZSM-5 catalytic supports: inductive influence of various seeds and aluminosilicate gels on the physicochemical properties and catalytic dehydrogenative behavior. *Mater Chem Phys* **165**:55–65 (2015).
41. Zhao X, Wei L, Cheng S, Huang Y, Yu Y and Julson J, Catalytic cracking of camelina oil for hydrocarbon biofuel over ZSM-5-Zn catalyst. *Fuel Process Technol* **139**:117–126 (2015). https://doi.org/10.1016/j.fuproc.2015.07.033.
42. Gurdeep Singh HK, Yusup S, Quitain AT, Abdullah B, Ameen M, Sasaki M *et al*., Biogasoline production from linoleic acid via catalytic cracking over nickel and copper-doped ZSM-5 catalysts. *Environ Res* **186**:109616 (2020). https://doi.org/10.1016/j.envres.2020.109616.
43. Aghajari N, Ghasemi Z, Younesi H and Bahramifar N, Synthesis, characterization and photocatalytic application of Ag-doped Fe-ZSM-5@ TiO2 nanocomposite for degradation of reactive red 195 (RR 195) in aqueous environment under sunlight irradiation. *J Environ Health Sci Eng* **17**(1):219–232 (2019).
44. den Breejen JP, Radstake PB, Bezemer GL, Bitter JH, Frøseth V, Holmen A *et al*., On the origin of the cobalt particle size effects in Fischer–Tropsch catalysis. *J Am Chem Soc* **131**(20):7197–7203 (2009). https://doi.org/10.1021/ja901006x.
45. Varvoutis G, Lykaki M, Stefa S, Binas V, Marnellos GE and Konsolakis M, Deciphering the role of Ni particle size and nickel-ceria interfacial perimeter in the low-temperature CO2 methanation reaction over remarkably active Ni/CeO2 nanorods. *Appl Catal Environ* **297**:120401 (2021). https://doi.org/10.1016/j.apcatb.2021.120401.
46. Lee K, Choi B, Lee C and Oh K, Effects of SiO2/Al2O3 ratio, reaction atmosphere and metal additive on de-NOx performance of HC-SCR over Cu-based ZSM-5. *J Ind Eng Chem* **90**:132–144 (2020).
47. Vitale G, Molero H, Hernandez E, Aquino S, Birss V and Pereira-Almao P, One-pot preparation and characterization of bifunctional Ni-containing ZSM-5 catalysts. *Appl Catal Gen* **452**:75–87 (2013). https://doi.org/10.1016/j.apcata.2012.11.026.
48. Long X, Zhang Q, Liu Z-T, Qi P, Lu J and Liu Z-W, Magnesia modified H-ZSM-5 as an efficient acidic catalyst for steam reforming of dimethyl ether. *Appl Catal Environ*


© 2023 The Authors. *Biofuels, Bioproducts and Biorefining* published by Society of Industrial Chemistry and John Wiley & Sons Ltd.


19321031, 2024, 3, Downloaded from https://scijournals.onlinelibrary.wiley.com/doi/10.1002/bbb.2536 by South African Medical Research, Wiley Online Library on [27/08/2024]. See the Terms and Conditions (https://onlinelibrary.wiley.com/terms-and-conditions) on Wiley Online Library for rules of use; OA articles are governed by the applicable Creative Commons License

**134**-**135**:381–388 (2013). https://doi.org/10.1016/j.apcatb.2013.01.034.
49. Xiong W *et al*., Performance of hierarchical ZSM-5 supported cobalt catalyst in the Fischer-Tropsch synthesis. *J Fuel Chem Technol* **45**(8):950–955 (2017).
50. Li X, Rezaei F and Rownaghi AA, Methanol-to-olefin conversion on 3D-printed ZSM-5 monolith catalysts: effects of metal doping, mesoporosity and acid strength. *Microporous and Mesoporous Materials* **276**:1–12 (2019). https://doi.org/10.1016/j.micromeso.2018.09.016.
51. Schultz EL, Mullen CA and Boateng AA, Aromatic hydrocarbon production from eucalyptus urophylla pyrolysis over several metal-modified ZSM-5 catalysts. *Energ Technol* **5**(1):196–204 (2017).
52. Valencia D and Klimova T, Citric acid loading for MoS2-based catalysts supported on SBA-15. New catalytic materials with high hydrogenolysis ability in hydrodesulfurization. *Appl Catal Environ* **129**:137–145 (2013).
53. Qi G and Yang RT, Ultra-active Fe/ZSM-5 catalyst for selective catalytic reduction of nitric oxide with ammonia. *Appl Catal Environ* **60**(1–2):13–22 (2005).
54. Wei Q, Zhang P, Liu X, Huang W, Fan X, Yan Y *et al*., Synthesis of Ni-modified ZSM-5 zeolites and their catalytic performance in n-octane hydroconversion. *Front Chem* **8**:586445 (2020).
55. Wu L, Li Y, Fu Z and Su B-L, Hierarchically structured porous materials: synthesis strategies and applications in energy storage. *Natl Sci Rev* **7**(11):1667–1701 (2020).
56. Zhang C, Fan K, Ma G, Lei C, Xu W, Jiang J *et al*., Efficient synthesis of mesoporous nano ZSM-5 zeolite crystals without a mesoscale template. *Crystals* **11**(10):1247 (2021).
57. Ji K, Xun J, Liu P, Song Q, Gao J, Zhang K *et al*., The study of methanol aromatization on transition metal modified ZSM-5 catalyst. *Chin J Chem Eng* **26**(9):1949–1953 (2018). https://doi.org/10.1016/j.cjche.2018.03.024.
58. Rostamizadeh M, Yaripour F and Hazrati H, Ni-doped high silica HZSM-5 zeolite (Si/Al = 200) nanocatalyst for the selective production of olefins from methanol. *J Anal Appl Pyrolysis* **132**:1–10 (2018). https://doi.org/10.1016/j.jaap.2018.04.003.
59. Seemala B and Wyman CE, Relationship between ZSM-5 pore modifications and gallium proximity and liquid hydrocarbon number distribution from ethanol oligomerization. *Cat Sci Technol* **12**(15):4903–4916 (2022).
60. Wan BZ and Yang TC, Preparation and catalytic properties of transition metal doped ZSM-5 zeolites. *J Chin Chem Soc* **37**(3):255–263 (1990).
61. Sousa ZS, Veloso CO, Henriques CA and da Silva VT, Ethanol conversion into olefins and aromatics over HZSM-5 zeolite: influence of reaction conditions and surface reaction studies. *J Mol Catal A Chem* **422**:266–274 (2016).
62. Zhang D, Wang R and Yang X, Effect of P content on the catalytic performance of P-modified HZSM-5 catalysts in dehydration of ethanol to ethylene. *Catal Lett* **124**(3):384–391 (2008).
63. Ramasamy KK, Zhang H, Sun J and Wang Y, Conversion of ethanol to hydrocarbons on hierarchical HZSM-5 zeolites. *Catal Today* **238**:103–110 (2014).
64. Ouyang J, Kong F, Su G, Hu Y and Song Q, Catalytic conversion of bio-ethanol to ethylene over La-modified HZSM-5 catalysts in a bioreactor. *Catal Lett* **132**(1):64–74 (2009).
65. Li Z, Lepore AW, Salazar MF, Foo GS, Davison BH, Wu Z *et al*., Selective conversion of bio-derived ethanol to renewable BTX over Ga-ZSM-5. *Green Chem* **19**(18):4344–4352 (2017).
66. Bi J, Guo X, Liu M and Wang X, High effective dehydration of bio-ethanol into ethylene over nanoscale HZSM-5 zeolite catalysts. *Catal Today* **149**(1):143–147 (2010). https://doi.org/10.1016/j.cattod.2009.04.016.
67. Zhan N, Hu Y, Li H, Yu D, Han Y and Huang H, Lanthanum–phosphorous modified HZSM-5 catalysts in dehydration of ethanol to ethylene: a comparative analysis. *Catal Commun* **11**(7):633–637 (2010). https://doi.org/10.1016/j.catcom.2010.01.011.
68. Sheng Q, Ling K, Li Z and Zhao L, Effect of steam treatment on catalytic performance of HZSM-5 catalyst for ethanol dehydration to ethylene. *Fuel Process Technol* **110**:73–78 (2013). https://doi.org/10.1016/j.fuproc.2012.11.004.
69. Ramasamy KK and Wang Y, Ethanol conversion to hydrocarbons on HZSM-5: effect of reaction conditions and Si/Al ratio on the product distributions. *Catal Today* **237**:89–99 (2014). https://doi.org/10.1016/j.cattod.2014.02.044.
70. Seifert M, Marschall MS, Gille T, Jonscher C, Busse O, Paasch S *et al*., Ethanol to aromatics on modified H-ZSM-5 part I: interdependent dealumination actions. *ChemCatChem* **12**(24):6301–6310 (2020). https://doi.org/10.1002/cctc.202001344.
71. Arjah A, Al-Bahar M, Li C and Garforth A, Selective cracking of light olefins to ethene and propene. *Chem Eng Trans* **57**:883–888 (2017).
72. Busto M, Vera CR and Grau JM, Optimal process conditions for the isomerization–cracking of long-chain n-paraffins to high octane isomerizate gasoline over Pt/SO42—ZrO2 catalysts. *Fuel Process Technol* **92**(9):1675–1684 (2011).
73. Kwak JH, Rousseau R, Mei D, Peden CHF and Szanyi J, The origin of regioselectivity in 2-butanol dehydration on solid acid catalysts. *ChemCatChem* **3**(10):1557–1561 (2011). https://doi.org/10.1002/cctc.201100173.
74. Roy S, Mpourmpakis G, Hong D-Y, Vlachos DG, Bhan A and Gorte RJ, Mechanistic study of alcohol dehydration on γ-Al2O3. *ACS Catal* **2**(9):1846–1853 (2012). https://doi.org/10.1021/cs300176d.
75. Janik MJ, Macht J, Iglesia E and Neurock M, Correlating acid properties and catalytic function: a first-principles analysis of alcohol dehydration pathways on polyoxometalates. *J Phys Chem C* **113**(5):1872–1885 (2009). https://doi.org/10.1021/jp8078748.
76. Yaripour F, Shariatinia Z, Sahebdelfar S and Irandoukht A, Conventional hydrothermal synthesis of nanostructured H-ZSM-5 catalysts using various templates for light olefins production from methanol. *J Nat Gas Sci Eng* **22**:260–269 (2015).
77. Rostamizadeh M, Boffito D, Patience G and Taeb A, Neural network modeling of methanol to propylene over P-ZSM-5 in a fluidized bed. *J Chem Proc Engg* **1**:1–8 (2014).
78. Li C, Ma J, Xiao Z, Hector SB, Liu R, Zuo S *et al*., Catalytic cracking of Swida wilsoniana oil for hydrocarbon biofuel over Cu-modified ZSM-5 zeolite. *Fuel* **218**:59–66 (2018).
79. Song Y, Zhang LL, Li GD, Shang YS, Zhao XM, Ma T *et al*., ZSM-5 extrudates modified with phosphorus as a super effective MTP catalyst: impact of the acidity on binder. *Fuel Process Technol* **168**:105–115 (2017).
80. Zheng A, Zhao Z, Chang S, Huang Z, Zhao K, Wu H *et al*., Maximum synergistic effect in the coupling conversion of bio-derived furans and methanol over ZSM-5 for enhancing aromatic production. *Green Chem* **16**(5):2580–2586 (2014).
81. Calsavara V, Baesso ML and Fernandes-Machado NRC, Transformation of ethanol into hydrocarbons on ZSM-5 zeolites modified with iron in different ways. *Fuel* **87**(8):1628–1636 (2008). https://doi.org/10.1016/j.fuel.2007.08.006.

© 2023 The Authors. *Biofuels, Bioproducts and Biorefining* published by Society of Industrial Chemistry and John Wiley & Sons Ltd.


19321031, 2024, 3, Downloaded from https://scijournals.onlinelibrary.wiley.com/doi/10.1002/bbb.2536 by South African Medical Research, Wiley Online Library on [27/08/2024]. See the Terms and Conditions (https://onlinelibrary.wiley.com/terms-and-conditions) on Wiley Online Library for rules of use; OA articles are governed by the applicable Creative Commons License

82. Vichaphund S, Aht-ong D, Sricharoenchaikul V and Atong D, Production of aromatic compounds from catalytic fast pyrolysis of jatropha residues using metal/HZSM-5 prepared by ion-exchange and impregnation methods. *Renew Energy* **79**:28–37 (2015).

**Ifeanyi Michael Smarte Anekwe**

Ifeanyi Michael Smarte Anekwe is currently completing his PhD studies in chemical engineering at the University of the Witwatersrand. His research focuses on the synthesis and characterization of a novel heterogeneous catalyst and its application in the conversion of low alcohols into fuel and petrochemicals. This groundbreaking work has already led to published articles. Given the increasing demand for sustainable energy and the need to reduce greenhouse gas emissions, his research is of great importance. He has presented his research findings at both global and local conferences. His research interests include heterogeneous catalysis, biofuel production, waste valorization, and biotechnology. His contributions span both sole and collaborative authorship, as well as his role as a reviewer for journals.

**Bilainu Oboirien**

Professor Bilainu Oboirien has a doctorate in chemical engineering from the University of the Witwatersrand. He is a full professor at the University of Johannesburg. His areas of research are the combustion and gasification of coal and biomass, $CO_2$ capture (oxy-fuel combustion and chemical looping combustion), waste-to-energy (waste tires and MSW gasification), and energy storage (power to gas, lithium ion batteries). He has co-authored 65 articles in high-impact journals in the field of energy and fuels and he is also a regular reviewer for journals.


© 2023 The Authors. *Biofuels, Bioproducts and Biorefining* published by Society of Industrial Chemistry and John Wiley & Sons Ltd.


19321031, 2024, 3, Downloaded from https://scijournals.onlinelibrary.wiley.com/doi/10.1002/bbb.2536 by South African Medical Research, Wiley Online Library on [27/08/2024]. See the Terms and Conditions (https://onlinelibrary.wiley.com/terms-and-conditions) on Wiley Online Library for rules of use; OA articles are governed by the applicable Creative Commons License